Study of high-precision earth sensor with triple-FOV

WANG Hongjian[1,2,3], XING Fei[1,2,3], YOU Zheng[1,2,3], CHU Daping[4], ZHENG Lungui[5]

(1.*Collaborative Innovation Center for Micro/Nano Fabrication, Device and System, Tsinghua University, Beijing* 100084, *P. R. China*

2.*State Key Laboratory of Precision Measurement Technology and Instruments, Tsinghua University, Beijing* 100084, *P.R.China*

3.*Department of Precision Instruments, Tsinghua University, Beijing* 100084, *P.R.China*

4.*Department of Engineering, Electrical Engineering Division, University of Cambridge, Cambridge CB*3 0*FA*, *U.K.*

5.*School of Instrument and Electronics, North University of China, Taiyuan* 030051, *P.R.China*)

Abstract: Earth sensors are widely used in spacecraft for attitude determination. They need to have a very large field of view (FOV) (>120°) and relatively low accuracy while being used in the aircrafts around orbit. A triple-FOV infrared earth sensor is proposed in this paper. It uses three pieces of standard infrared detectors with a wavelength range of 14 ~ 16μm, to sense the horizontal circle by detecting the infrared light emitted from the earth. From which, the geocentric vector can be obtained. A mathematic model is established and a validation model is set up to provide input parameters for the mathematic model. The simulation results of the two models show that the output of the mathematic model coincides with the known parameters. Based on the above analysis, a prototype has been built and tested. The test results show that the angle measurement error is about 0.002° and hence such a triple-FOV earth sensor is capable to provide high-precision position information for autonomous navigation.

Key words: Earth Sensor, Validation Model, High Precision, Autonomous Navigation

1 Introduction

Earth sensor is an important subsystem of the attitude determination and control systems used in spacecraft.[1-3] It observes the discontinuity between the earth and the space to obtain the horizontal circle. Then, the geocentric vector can be determined [4-7]. It is well known that infrared earth sensors can be divided into two categories, static ones and dynamic scanning ones, based on their working principle. Although the technology of dynamic scanning earth sensors [8-10] is relatively mature, its life expectancy and development are subject to various restrictions. While static earth sensors have the advantages in quality, power, accuracy and life expectancy. Thus, it has gradually become the focus of research. [11-14]

A triple-FOV earth sensor based on standard infrared detectors is proposed to meet the requirement of being used in aircrafts around earth orbit. It can work out the geocentric vector and calculate the altitude of an aircraft by sensing the horizontal circle through the atmosphere radiation in the wavelength range of 14 ~ 16μm, which can make sure that such an earth sensor is capable to operate normally day and night regardless of the weather condition and the light impact [15-17].

2 Mathematic Model

A mathematic model of triple-FOV earth sensor is established based on the use of linear CCDs. As shown in Figure 1, three optical axes are set as 120° from each other, and q_0 is a structural parameter between the optical axis and z_{es}.

As shown in Figure 2, the initial coordinate frame is set as $x_1y_1z_1$. Then, the coordinate frame rotates in turn of z-axis, x-axis and y-axis with an angle of α, β and γ, respectively. Finally, $x_2y_2z_2$ and the coordinate transformation matrix can be calculated.

Considering that the vector to the Earth centre is $\vec{E}_{11} = [0, 0, -1]^T$ in $x_1y_1z_1$ frame, the geocentric vector in the new coordinate frame can be expressed as follows by using the transformation matrix, while α can be set as 0.

$$\vec{E}_{21}=[\cos\beta\sin\gamma - \sin\beta - \cos\beta\cos\gamma]^{T} \quad (1)$$

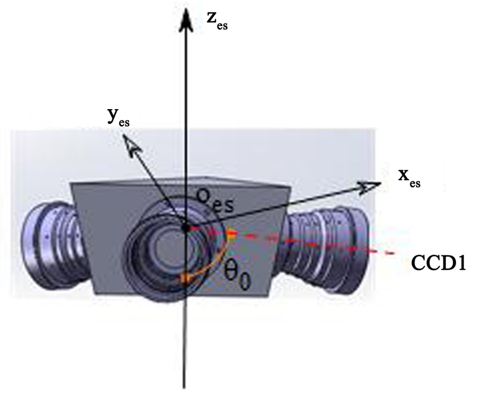

Fig. 1 Earth sensor coordinate frame

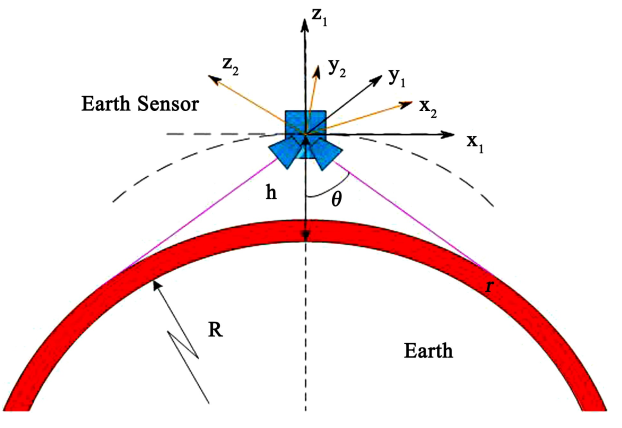

Fig. 2 Mathematic model

The center vector $\vec{E}_{22}$ in $x_2y_2z_2$ frame can be expressed by three vectors, $\vec{X}_{21}$ $\vec{X}_{22}$ $\vec{X}_{23}$, from the earth sensor to the edge. Upon the analysis above, the following equation can be obtained.

$$\vec{E}_{21}=\vec{E}_{22} \quad (2)$$

So β and γ can be expressed as follows.

$$\sin\beta = -\vec{E}_{22}(2)$$

$$\tan\gamma = -\frac{\vec{E}_{22}(1)}{\vec{E}_{22}(3)} \quad (3)$$

Thus, h can be expressed as follows.

$$h=\frac{R+r}{\sqrt{1-(\cos\beta)^2\cdot(\cos(\theta_0-\varphi_1-\gamma))^2}}-R \quad (4)$$

where $\varphi_1=\arctan(\frac{u_1}{f})$, u_1 the signal point in the CCD1 coordinate frame, r the thickness of the carbon dioxide absorption belt in the 14 ~ 16 μm range, R is the radius of the earth.

3 Validation Model

As shown in Figure 3, the initial state of the earth sensor is set as a fixed coordinate frame $o_g-x_gy_gz_g$. After rotating at the turn 3-1-2, it becomes a new coordinate frame $o_{es}-x_{es}y_{es}z_{es}$, where $o_gF_1B_1F_2$ is the conical surface of observing the earth infrared horizon by earth sensor.

The relationship between the altitude h and half cone angle q can be expressed as follows:

$$\sin\theta=\frac{R+r}{R+h} \quad (6)$$

The conical surface equation can be expressed as follows:

$$z=-k\sqrt{x^2+y^2} \quad (7)$$

where $k=\cot\theta$.

The extension lines of three linear detectors intersect at one point in z_{es} axis. $o_{es}o_{f1}$ is a parameter and set as $o_{es}o_{f1}=o_{es}o_{f2}=o_{es}o_{f3}=a$.

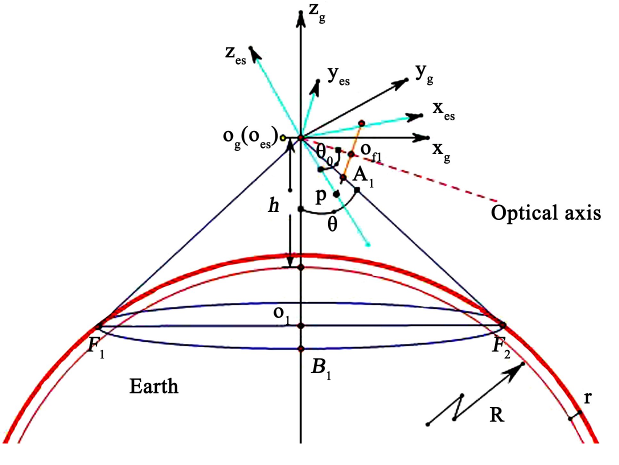

Fig. 3 Validation model

As shown in Figure 3, the linear parametric equations $p_go_{f1,g}$, $p_go_{f2,g}$ and $p_go_{f3,g}$ can be obtained as follows:

$$\begin{cases} x=t_m(x_{ofm,g}-x_{pg})+x_{pg} \\ y=t_m(y_{ofm,g}-y_{pg})+y_{pg} \\ z=t_m(z_{ofm,g}-z_{pg})+z_{pg} \end{cases} \quad (8)$$

where tm>0 and m=1,2,3.

After solving the equations between the linear parametric equations and the conical surface equation, the signal point $A'_{m,g}$ (m=1,2,3) can be obtained.

However, the signal point $A_{m,g}$ can also be expressed after the coordinate transformation from $A_{m,fm}$ in the CCD coordinate frame f_m (m=1,2,3) .

Since $A'_{m,g}$ is equal to $A_{m,g}$, the signal point coordinates u_1 u_2 u_3 in the CCD coordinate frame can be obtained as follows.

$$u_1=-\frac{[t_1(x_{of1,g}-x_{pg})+x_{pg}+a\cos\beta\cos(\theta_0-\gamma)]}{\sin\theta_0\cos\gamma-\cos\theta_0\sin\gamma}$$

$$u_2=-\frac{[t_2(x_{of2,g}-x_{pg})+x_{pg}-\cos(\frac{2\pi}{3})a\sin\theta_0\cos\gamma+a\cos\theta_0\sin\gamma]}{\cos(\frac{2\pi}{3})\cos\theta_0\cos\gamma+\sin\theta_0\sin\gamma}$$

$$u_3=-\frac{[t_3(x_{of3,g}-x_{pg})+x_{pg}-\cos(\frac{4\pi}{3})a\sin\theta_0\cos\gamma+a\cos\theta_0\sin\gamma]}{\cos(\frac{4\pi}{3})\cos\theta_0\cos\gamma+\sin\theta_0\sin\gamma} \tag{9}$$

4 Simulation Analysis

4.1 Simulation between two models

Among the parameters in use, h changes from 50km to 100km, r is set to be 20km, R is 6370km, a is 0.05m, and β and γ change from -10° to +10° respectively. With the above parameters as the input to the validation model, u_1, u_2, u_3 can be obtained correspondingly. Figure 4 to Figure 6 show that u_1, u_2 and u_3 change with β, γ and h, respectively.

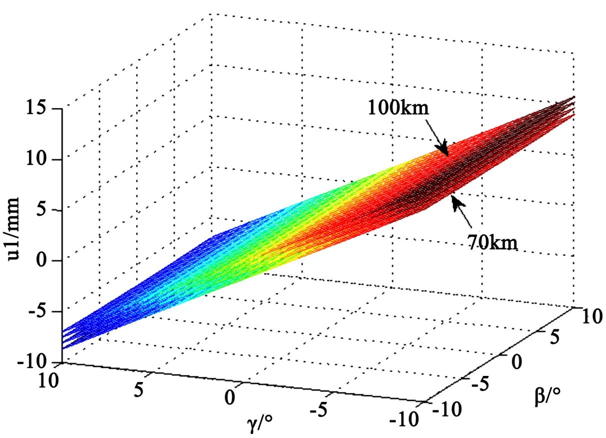

Fig. 4 u_1 changes with β, γ and h

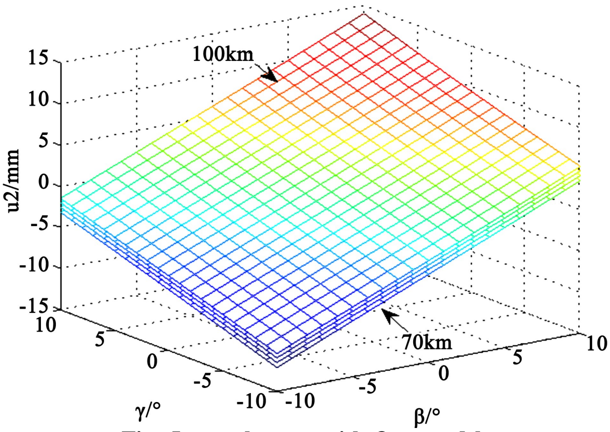

Fig. 5 u_2 changes with β, γ and h

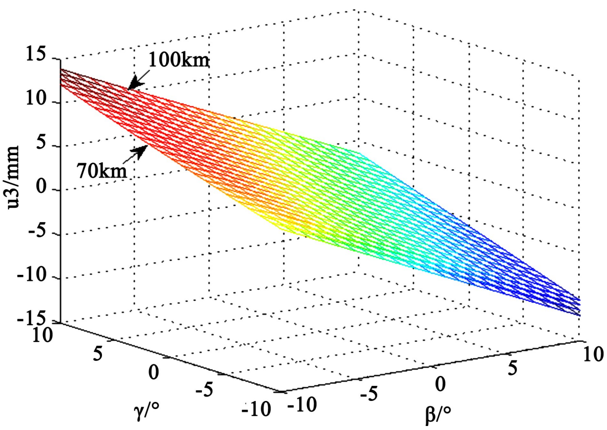

Fig. 6 u_3 changes with β, γ and h

Take u_1, u_2 and u_3 as input parameters of the mathematic model. The altitude h, roll angle β and pitch angle γ can be obtained respectively. Figure 7 to Figure 9 show that h, β and γ change with u_1, u_2 and u_3, respectively.

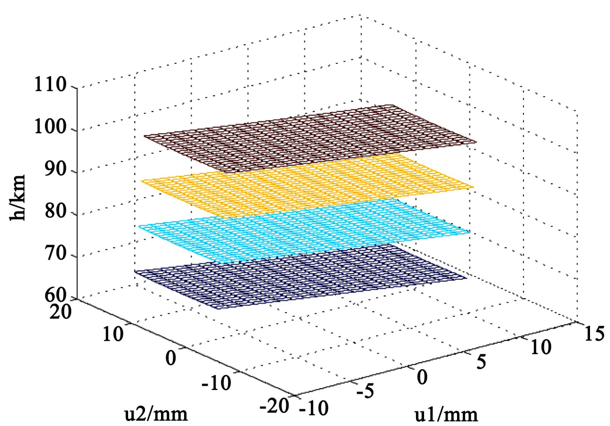

Fig. 7 h changes with u_1, u_2 and u_3

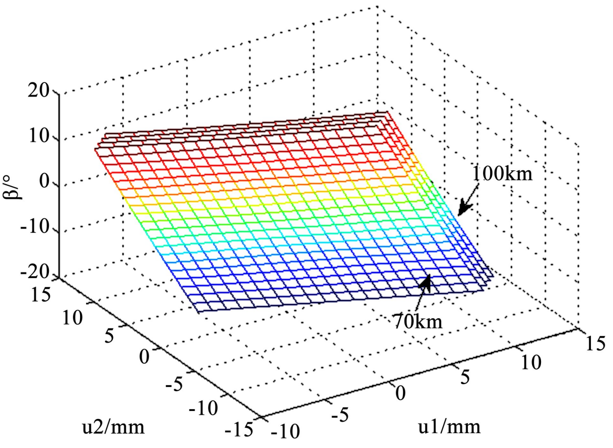

Fig. 8 β changes with u_1, u_2 and u_3

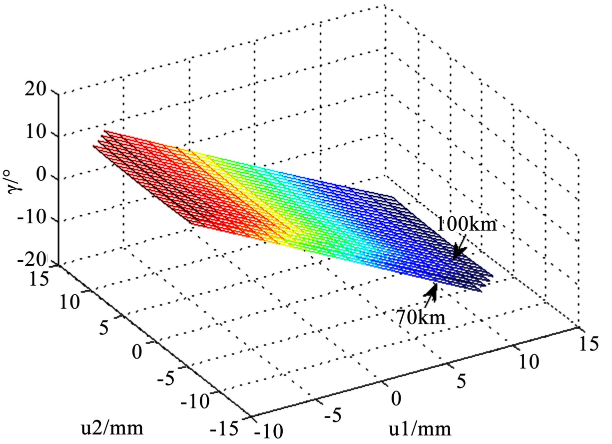

Fig. 9 γ changes with u_1, u_2 and u_3

The simulation results show that the output of mathematic model coincides with the known parameters well, that is, the validation model can provide suitable input parameters for the mathematic model.

4.2 Detection accuracy simulation

When the extraction points on the detectors have errors, u_1, u_2 and u_3 will have an effect on the results of height measurement and attitude determination. Assuming that the signal extraction error is 0.1 pixel, there are eight situations as shown in Table 1, where u_{10}, u_{20} and u_{30} are known points.

The results of β, γ and h are shown in Table 2, where the measurement error of h is about 13.358m and the attitude measurement error is about 0.001°.

Table 1 Eight situations of u_1, u_2 and u_3 with error

	u_1	u_2	u_3
1	u_{10}+ 0.1 pixel	u_{20}+ 0.1 pixel	u_{30}+ 0.1 pixel
2	u_{10}+ 0.1 pixel	u_{20}+ 0.1 pixel	u_{30}- 0.1 pixel
3	u_{10}+ 0.1 pixel	u_{20}- 0.1 pixel	u_{30}+ 0.1 pixel
4	u_{10}+ 0.1 pixel	u_{20}- 0.1 pixel	u_{30}- 0.1 pixel
5	u_{10}- 0.1 pixel	u_{20}+ 0.1 pixel	u_{30}+ 0.1 pixel
6	u_{10}- 0.1 pixel	u_{20}+ 0.1 pixel	u_{30}- 0.1 pixel
7	u_{10}- 0.1 pixel	u_{20}- 0.1 pixel	u_{30}+ 0.1 pixel
8	u_{10}- 0.1 pixel	u_{20}- 0.1 pixel	u_{30}- 0.1 pixel

Table 2 β, γ and h change with different situations of u_1, u_2 and u_3

	β/°	γ/°	h/m
1	0.0000	0.0000	13.3583
2	0.0011	−0.0006	4.7473
3	−0.0011	−0.0006	4.7473
4	0.0000	−0.0012	−3.8629
5	0.0000	0.0012	4.7473
6	0.0011	0.0006	−3.8629
7	−0.0011	0.0006	−3.8629
8	0.0000	0.0000	−12.4724

5 Test

Based on the analysis above, a test is conducted to confirm the validation model and the accuracy of the earth sensor. As shown in Figure 10, the earth sensor is fixed on the turntable. The brightness of the collimator was adjusted, and the turntable was rotated to make sure that the earth sensor can detect the incident ray from the collimator.

Fig. 10 Experiment setup

As the turntable rotates from −0.498° to 0.500° with 0.002° step for each rotation, the relationship between the gray values and different pixels of the linear CCD is shown in Figure 11. After normalizing the gray values, linear fitting is applied to each curve and the results are shown in Figure 12.

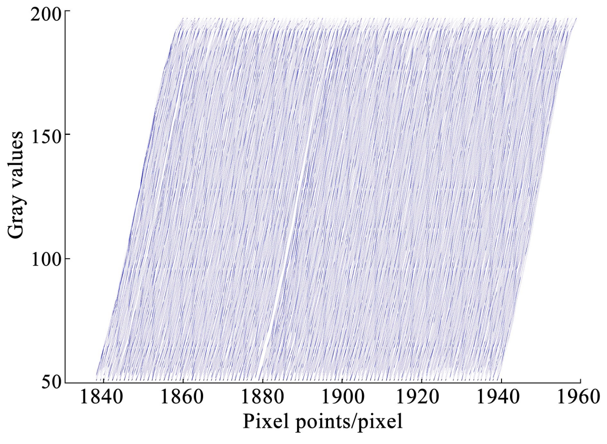

Fig. 11 The relationship between gray values and different pixels

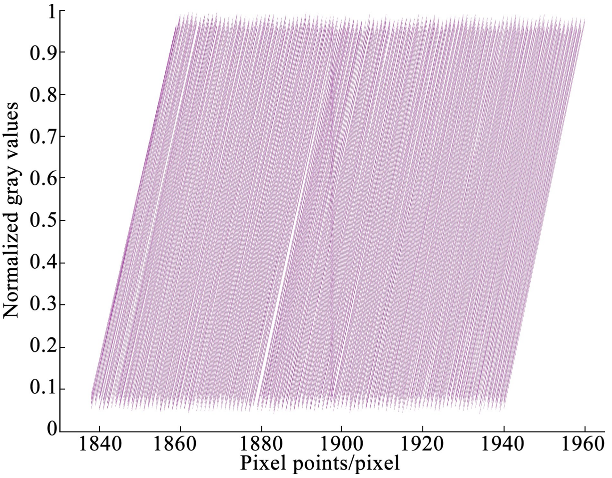

Fig. 12 Fitted curves

Taking the gray values of 1845 ~ 1855 pixels of the first curve as a reference, pixel values of the other linear fitting curves at the same gray value are calculated and the pixel difference between the adjacent curves are obtained. The averaged value and standard deviation of the pixel difference at a gray value are shown in Table 3, where the average is about 0.2 pixel and the standard deviation is about 0.05 pixel respectively.

As a result, when the earth sensor rotates 0.002°, the signal point will change about 0.2 pixel.

Table 3 The averaged value and standard deviation of pixel difference between the adjacent curves

Pixel	Average of pixel difference	Standard deviation of pixel difference
1845	0.2053	0.0464
1846	0.2055	0.0443
1847	0.2048	0.0436
1848	0.2047	0.0440
1849	0.2040	0.0456
1850	0.2043	0.0483
1851	0.2039	0.0514
1852	0.2030	0.0550
1853	0.2002	0.0577
1854	0.1976	0.0584
1855	0.1956	0.0608
Average	0.2026	0.0505

6 Conclusion

Aiming for the use in aircrafts around the earth orbit, a triple-FOV earth sensor is proposed and simulated. A validation model is established to provide input parameters for the earth sensor and a way to test the earth sensor. A prototype is built and tested in laboratory. The simulation and testing results show that the attitude measurement error is about 0.002°. This shows that the earth sensor proposed in this paper can provide high-precision information for aircrafts to achieve autonomous navigation.

Acknowledgements

This work was financially supported by the National High Technology Research and Development Program of China (863 Program) (No. 2012AA121503 and No. 2012AA120603), the National Natural Science Foundation of China (No. 61377012) and the Tsinghua University Initiative Scientific Research Program (No.20131089242).

References

[1] YANG X L, ZHAO J H, WANG T B, et al. The Design for Electrical Signal Source of Infrared Earth-Wave [C]. 7th International Symposium on Instrumentation and Control Technology: Measurement Theory and Systems and Aeronautical Equipment, 2008, 7128(71282E).

[2] HANEL R A, BANDEEN W R, CONRATH B J. The infrared horizon of the planet earth [J]. Journal of the Atmospheric Sciences, 1963,20(2):73-86.

[3] CHORY M A, HOFFMAN D P, LEMAY J L. Satellite autonomous navigation-status and history, 1986 [C].1986.

[4] SOTO-ROMERO G, FOURNIOLS J, VERGNENEGRE C, et al. Uncooled micro-earth sensor for microsatellite attitude control, 2000[C].2000.

[5] GEOFFRAY H, BARDOUX A, LAPORTE M, et al. Uncooled infrared microbolometer arrays for earth remote sensing [J]. Infrared Technology and Applications XXVI, 2000,4130:527-536.

[6] SOTO-ROMERO G, BONY F, SIMONNE J, et al. Micro Infrared Earth Sensor project: an integrated IR camera for Earth remote sensing [J]. Proceedings of SPIE, 2001, 4540:176-187.

[7] ALBUKERQUE J, MATHET F, POCHARD M, et al. Development of static Earth horizon sensors, 2003 [C].2003.

[8] TEKAWY J A, WANG P, GRAY C W. Scanning horizon sensor attitude correction for earth oblateness [J]. Journal of guidance, control, and dynamics, 1996,19(3):706-708.

[9] LI J. Simple Correction algorithm of scanning horizon sensor measurement for earth oblateness [J]. Journal of guidance, control, and dynamics, 1999, 22(1): 187-190.

[10] HABLANI H B. Roll/pitch determination with scanning horizon sensors-Oblateness and altitude corrections [J]. Journal of Guidance Control and Dynamics, 1995,18(6):1355-1364.

[11] ROGALSKI A. Infrared detectors: an overview [J]. Infrared Physics & Technology, 2002,43(3 - 5):187-210.

[12] LIBERATI F, PERROTTA G, VERZEGNASSI F. Low cost Earth Attitude Sensor: Proceedings of the 5th International Conference on Space Optics (ICSO 2004), Toulouse, France, 2004[C].30 March - 2 April 2004.

[13] GUOQUAN S, HAO W, ZHENDONG G, et al. Design of Infrared Static Focal Plane Earth Sensor for Micro-Satellite [J]. Chinese Journal of Sensors and Actuators, 2012,25.

[14] XIANGHUA X. Study on Micro-satellite Attitude Control System [D]. Nanjing University of Aeronautics and Astronautics, 2007.

[15] SHU G. Research of the Measuring Method Whit Time Constant of Infrared Probe Based on 14-16. 25 [D]. Changchun University of Science and Technology, 2012.

[16] CHANGSHUI C, RONGTING L, SONGHAO L. New Development of Infrared Detector [J]. Journal of Atmospheric and Environmental Optics, 2013:1-10.

[17] SONNENFROH D, PARAMESWARANA K, BRUNOB J, et al. Advanced sensors for Earth-sciences applications [C]. Proc. of SPIE, 2013,8631.

Authors' Biographies

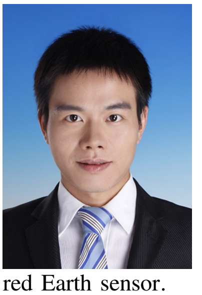

WANG Hongjian, born in 1987, is currently a Ph.D. candidate in the Department of Precision Instruments, Tsinghua University (THU), China. He obtained his B.A. degree from THU in 2010. His research interests include celestial navigation technology and infrared Earth sensor.

E-mail: wanghongjian@tsinghua.org.cn

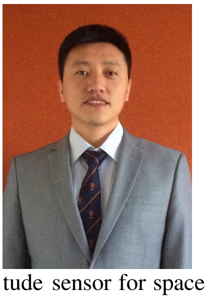

XING Fei, born in 1979, is currently an associate professor in Tsinghua University, China. He received his Bachelor degree from Tongji University in 2002 and Ph.D. degree from Tsinghua University in 2007. His current research interests focus on advance optical attitude sensor for space, remote sensing and celestial navigation.

Email: xingfei@tsinghua.edu.cn

YOU Zheng, born in 1963, is an Academician of Chinese Academy of Engineering, and a Professor of Chang Jiang Scholar in Tsinghua University, China. He is also the Assistant President of Tsinghua University, the Dean of the School of Mechanical Engineering and

the Chairman of the Department Precision Instrument. Respectively. His current research includes MNT technology, Micro/Nano satellite technology and their applications.
Email: yz-dpi@tsinghua.edu.cn

CHU Daping, is the Chairman of CAPE (Centre for Advanced Photonics and Electronics) and Head of Photonics and Sensors Group in Cambridge University Engineering Department. Current research includes space light modulation and phase-only holography for displays and imaging as well as optical communications, laminated electro-active foils for solar shading and smart facade, and high frequency tuneable dielectrics for GHz/THz applications.
Email: dpc31@cam.ac.uk

ZHENG Lungui, born in 1980, is currently a lecturer in the School of Instrument and Electronics, North University of China. He obtained his Ph.D. degree from Tsinghua University in 2014. His research interests include strapdown inertial navigation system and integrated navigation.
E-mail: menock1994@sina.com